ADVANCED ELECTRONIC MATERIALS
www.advelectronicmat.de

Trap-Assisted Triplet Emission in Ladder-Polymer-Based Light-Emitting Diodes

*Elham Khodabakhshi, Charusheela Ramanan, Jasper J. Michels, Sven Bonus, Dirk Hertel, Klaus Meerholz, Michael Forster, Ulrich Scherf, and Paul W. M. Blom**

The charge transport and recombination in light-emitting diodes (LEDs) based on a methyl-substituted poly(*p*-phenylene) ladder polymer (Me-LPPP) are investigated. The transport is characterized by a high room-temperature hole mobility of 2×10^{-8} m^2 V^{-1} s^{-1} combined with anomalously strong electron trapping. Their electroluminescence (EL) spectrum is characterized by a blue singlet emission, a broad green featureless peak, and a yellow-orange triplet emission. The voltage dependence of the EL spectrum and negative contribution to the capacitance indicate that the triplet-emission is of trap-assisted nature, consistent with the strong electron trapping. Consequently, the color purity of the blue emissive Me-LPPP polymer LEDs can be strongly improved using trap dilution.

1. Introduction

Conjugated polymers are of considerable interest as potential active materials in organic electronic applications such as polymeric light-emitting diodes (PLEDs), plastic lasers, photovoltaic devices (solar cells), and field-effect transistors.[1–5] One of the main goals of materials development for OLEDs is obtaining stable pure blue emission, which is required for full-color displays, combined with good charge transporting properties.[6–10] However, charge transport in organic semiconductors is typically reduced by energetic disorder and trapping sites due to defects.[11] Ladder-type poly(*p*-phenylene) polymers (LPPP) are an interesting class of conjugated polymers due to their purity and low degree of structural and energetic disorder.[12] The reduced disorder is reflected in the sharp spectral features of the absorption and fluorescence spectra as well as a low amount of aggregate formation that could lead to trapping.[13] Time-of-flight measurements revealed that the hole transport in ladder-type methyl-substituted poly(*p*-phenylene) (Me-LPPP) is non-dispersive, combined with a hole mobility in the 10^{-7} m^2 V^{-1} s^{-1} range, which is much larger as compared to other poly(*p*-phenylene vinylene) (PPV) derivatives.[14] The very small dependence of the mobility on temperature furthermore reflects the small inhomogeneous width of the density of states (DOS) as a result of reduced disorder.

Next to blue singlet emission, this class of materials also exhibits some additional spectral features at higher wavelengths. At low temperatures, triplet emission has been observed using gated detection.[15] The observed phosphorescence spectrum was shifted with respect to the fluorescence spectrum by ≈0.6 eV and exhibited similar vibronic replica. Furthermore, a featureless broad excimer-like band was observed at an intermediate energy with respect to the fluorescent and phosphorescent spectra. In a later study, electrically induced phosphorescence even at room temperature was found in a diaryl (diphenyl)-substituted LPPP derivative.[16] It was proposed that the room temperature phosphorescence was the result of triplet diffusion toward sites where residual traces of palladium are covalently bound to the polymer. Probing the sensitivity of the spectra to oxygen confirmed that the phosphorescent features were quenched by oxygen, whereas the broad featureless peak got stronger.[16] The latter indicates that this broad peak is the result of oxidative defects similar to fluorenone in polyfluorenes (PFO), as also reported in later studies on LPPP polymers.[17–19]

In spite of extensive optical characterization, the device operation of LPPP-based PLEDs has not been addressed so far. In this study, we address the electron and hole transport of Me-LPPP as well as the voltage dependence of the electroluminescence (EL) spectra of Me-LPPP-based PLEDs. We observe that the electron current is severely limited by trapping, which leads to highly unbalanced charge transport. Similar to Lupton et al.,[16] we also observe room temperature electro-phosphorescence

Dr. E. Khodabakhshi, Dr. C. Ramanan, Dr. J. J. Michels, Prof. P. W. M. Blom
Department of Molecular Electronics
Max Planck Institute for Polymer Research
Ackermannweg 10, Mainz 55128, Germany
E-mail: blom@mpip-mainz.mpg.de
S. Bonus, Dr. D. Hertel, Prof. K. Meerholz
Institute of Physical Chemistry
University of Cologne
Greinstrasse 4-6, Cologne 50939, Germany
M. Forster, Prof. U. Scherf
Institute for Polymer Technology
Bergische Universität Wuppertal
Gaußstraße 20, Wuppertal 42119, Germany
The ORCID identification number(s) for the author(s) of this article can be found under https://doi.org/10.1002/aelm.202000082.

DOI: 10.1002/aelm.202000082

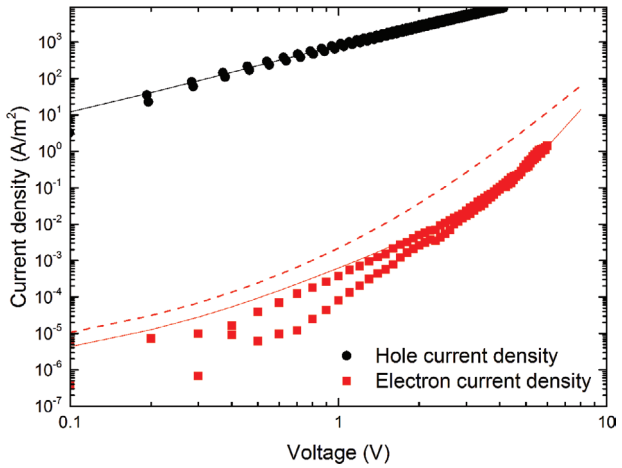

Figure 1. Hole and electron current density versus voltage for Me-LPPP hole- and electron-only devices. Symbols are experimental results; the solid lines are fits using EGDM (free electrons and holes) and electron traps consisting of universal electron traps (dashed line) and an additional single-level trap (solid line). The inset shows the chemical structure of Me-LPPP with $R_1 = n\text{-}C_6H_{13}$ and $R_2 = 1,4\text{-}(C_6H_4)\text{-}n\text{-}C_{10}H_{21}$.

for Me-LPPP. The electroluminescence spectra are strongly dependent on the bias voltage, with the relative contribution of the phosphorescent triplet emission being weakened at higher bias. Such behavior is characteristic for trap-assisted recombination. The presence of trap-assisted triplet emission is further manifested by a negative contribution to the PLED capacitance. The trap-assisted character of the triplet-emission allows us to completely suppress the phosphorescence using trap dilution by blending Me-LPPP with low-molecular-weight polystyrene (PS), resulting in pure blue emission.

2. Results and Discussion

2.1. Single-Carrier Devices

Understanding the operation of PLEDs requires a thorough characterization of charge transport, charge injection, and recombination mechanisms. Single-carrier devices are excellently suited for exploring the hole and electron transport independently. Hence, as a first step, we study the electron and hole current in Me-LPPP-based single carrier devices, of which the device architecture is given in Experimental Section.

In **Figure 1**, the measured hole and electron current densities of Me-LPPP are plotted (symbols) as a function of voltage (log *J*–log *V*). The observed slope of two in the log *J*–log *V* plot for $V \geq 1$ V shows that, as has been observed for many semiconducting polymers,[20] the hole current is space-charge limited (quadratic dependence of current on voltage) and trap-free. Applying Childs law $J = \frac{9}{8}\varepsilon\mu\frac{V^2}{L^3}$, with ε the permittivity and μ the mobility, leads to an estimated room temperature hole mobility for Me-LPPP of 3×10^{-8} m² V^{-1} s^{-1} (Figure 1, solid black line). In order to gain more quantitative information on the hole transport in Me-LPPP, the hole-only devices were also measured at different temperatures (symbols in Figure S1a, Supporting Information). To model the trap-free hole current, the extended Gaussian disorder model (EGDM) was used that contains as relevant parameters μ_0, a mobility prefactor containing the electronic overlap between transport sites, the energetic disorder σ, and a, the average distance between two transport sites.[21,22] These parameters then define the dependence of mobility on temperature, charge carrier density, and electric field. From the modeling (solid lines in Figure S1a, Supporting Information), we found $\mu_0 = 120$ m² V^{-1} s^{-1}, $\sigma = 0.06$ eV, and $a = 2.5 \times 10^{-9}$ m. At room temperature and zero electric field, these parameters result in a hole mobility of 2×10^{-8} m² V^{-1} s^{-1}, which is one order of magnitude lower as compared to earlier time-of-flight data.[14] The weak temperature dependence, as also reported in literature,[14] originates from a low value for the energetic disorder of $\sigma = 0.06$ eV, which is significantly lower than values found for other PPV derivatives, typically ranging from $\sigma = 0.12$ to 0.15 eV.[21]

In contrast, the electron transport in Me-LPPP is strongly suppressed and exhibits a steeper voltage dependence, which is characteristic for trap-limited currents. Figure 1 reveals that for the Me-LPPP device, the hole- and electron current differ by nearly five orders of magnitude. Such a large difference is ten to hundred times larger than observed for other PPV derivatives[23,24] or PFO-based[10] semiconductors. In an earlier study, it has been reported that the electron current in conjugated polymers is mediated by universal electron traps, with a typical density of $\approx 5 \times 10^{23}$ m^{-3}.[20] The extraordinary low electron current observed in Me-LPPP could point to the fact that next to these universal traps additional trap centers are present in the band gap of Me-LPPP.

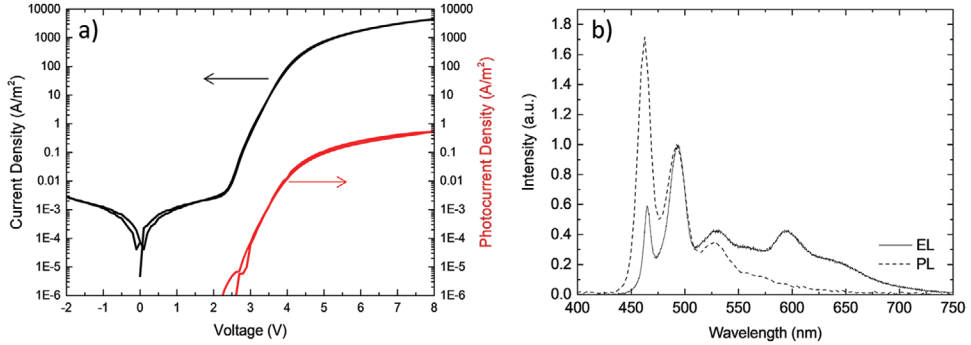

Figure 2. a) Current and photocurrent density of a PLED based on a 120 nm active layer of Me-LPPP. b) Electroluminescence spectrum (solid line) and photoluminescence spectrum (dash line) of the same device.

2.2. Steady State Electro- and Photoluminescence

As the next step, dual carrier devices were fabricated to investigate the recombination properties of the Me-LPPP-based PLEDs. **Figure** 2a shows the current and photocurrent density of the PLED. These characteristics correspond to an external quantum efficiency of 1%. Furthermore, Figure 2b shows the electroluminescence and photoluminescence (PL) spectra of Me-LPPP devices, normalized to the 0–1 peak. Both spectra exhibit the typical spectral PL characteristic of LPPPs: The S0-S1 (0-0) transition band of the PL spectrum peaks at 460 nm and is followed by a vibronic fine structure.[25] However, in the EL spectrum, the intensity of the 0–0 peak is much lower than the one in PL, which might originate from self-absorption. Besides the vibronic peaks of the singlet to ground state transition, the EL spectrum reveals two additional features observed at higher wavelength: i) a broad green emission band more or less centered around 560 nm and ii) a vibronically structured feature with a peak maximum at 590 nm. Strikingly, both features are absent in PL. As discussed in the introduction, the broad green emission at 560 nm may be due to the presence of a small amount of ketone defects, similar to PFO[10] or excimers.[15,26]

The second additional feature at 590 nm bears strong resemblance with the structured long wavelength emission observed in the EL spectrum measured for Ph-LPPP, which was ascribed to electrophosphorescence due to triplet diffusion toward covalently attached palladium centers, remaining in the material after the Suzuki polycondensation.[16] The lower emission intensity observed for the long wavelength feature for Me-LPPP compared to Ph-LPPP is consistent with the lower Pd content in our sample of ≈2 ppm, compared to 80 ppm for Ph-LPPP.[16] A question that arises is whether these Pd centers that give rise to triplet emission are also responsible for the anomalously low electron current in Me-LPPP. In that case, the triplet emission is expected to be of trap-assisted nature.

A typical fingerprint of trap-assisted recombination is that the EL spectrum is voltage dependent. In **Figure 3**, the EL spectrum is shown for various voltages (5–8 V). When normalized to the blue (singlet) bimolecular recombination, we observe that the triplet emission at higher wavelength is relatively weakened. There are two possible explanations for this negative voltage dependence: i) enhanced annihilation of triplets upon increasing the operating voltage as a result of an increase in excitation density,[16,27,28] and ii) emissive recombination of trapped electrons with free holes.[10] In case of the latter, since the number of trapping sites is fixed, the rate of trap-assisted recombination is only dependent on the hole density in the PLED, that is, linearly dependent on the charge carrier density. In contrast, the recombination rate of free electrons and holes leading to the blue singlet emission is bimolecular as it is a function of both the electron and holes density and hence quadratically dependent on the charge carrier density, making the blue bimolecular emission dominant at higher voltages. As a result of this difference in scaling of the trap-assisted and bimolecular (Langevin) recombination rates on the charge carrier density, the light emission resulting for these processes scales with the current density as $\approx J^{1/2}$ and $\approx J$.[29]

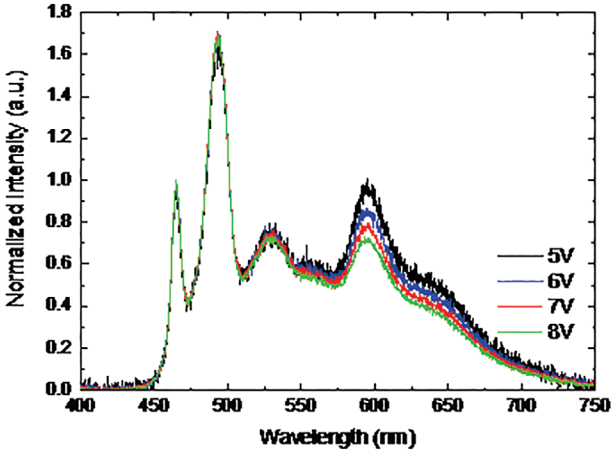

Figure 3. Voltage sweep of normalized electroluminescence spectra for a PLED with Me-LPPP as emissive layer.

To evaluate this further, we deconvoluted the EL spectra recorded at four different voltages (**Figure 4**a–d). The total emission was reconstructed by using three Gaussian peaks to describe the singlet spectrum, an additional peak for the broad green emission band (green line) centered at ≈2.2 eV, and two more (vibronic) peaks to account for the structured red emitting feature (red and blue lines). We note that the energy splitting between the latter is almost identical to the splitting of the zeroth and first vibronic transition in the singlet spectrum (i.e., ≈0.15 eV), which supports the triplet nature of the long wavelength feature.[16]

Plotting the peak area as a function of the current density for the red (1.8–2.2 eV) and blue (2.4–2.8 eV) regions of the emission spectrum on a double logarithmic scale produces lines with slopes of, respectively, ½ and 1, demonstrating the trap-assisted origin of the long wavelength emission feature (see **Figure 5**).

2.3. Impedance Spectroscopy

In order to further investigate the recombination mechanism in Me-LPPP-based PLEDs, we performed impedance spectroscopy (IS) measurements. IS is a powerful technique to study charge transport and recombination in semiconductors at different time scales.[30] In a recent study, it has been demonstrated that trap-assisted recombination gives rise to a negative contribution in the PLED capacitance.[31] For a single exponential transient recombination current, $J_r(t) = -J_0 \exp(-t/\tau_r)$ with J_0 the prefactor and τ_r the relaxation time, the capacitance is given by

$$C(\omega) = C_0 - \frac{\alpha\tau_r}{1+\omega^2\tau_r^2} \quad (1)$$

with C_0 the geometrical capacitance $\varepsilon_0\varepsilon_r A/d$, ω the angular frequency, and α a proportionality factor that scales with the PLED current density. The relaxation time τ_r observed in the IS spectra is a measure for the inverse rate for trap-assisted recombination. When only bimolecular recombination is present, by suppressing trap-assisted recombination using trap-dilution, the negative capacitance effect disappears.[31] As it can be observed in **Figure 6**, the capacitance of PLEDs based on Me-LPPP

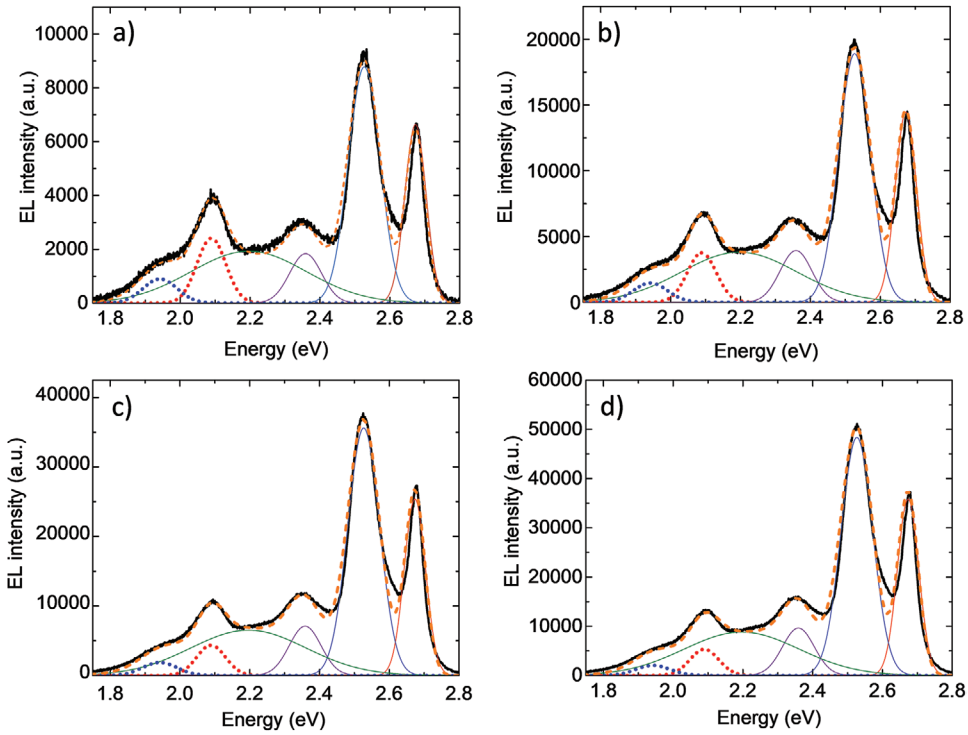

Figure 4. Deconvolution of EL Spectra recorded at various voltages: a) 5 V, b) 6 V, c) 7 V, and d) 8 V.

exhibits a very strong negative contribution compared to, for instance, typical PPV-based LEDs. This strong negative contribution is qualitatively consistent with the severe electron trapping observed in Me-LPPP (Figure 1). In PPV-based PLEDs, it was shown that the relaxation time τ_r is given by $\tau_r = \frac{2}{N_t C_p}$, with C_p representing the hole capture coefficient given by $(q/\varepsilon_0\varepsilon_r)\mu_p$, with μ_p the hole mobility, and N_t the total amount of electron traps. By applying Equation (1) to the experimental data with τ_r and α as fitting parameters, the frequency dependence of the capacitance at various voltages (Figure 6a) is fitted. We obtain a voltage-independent relaxation time τ_r of 20 ms for the Me-LPPP-based PLED. This time constant is orders of magnitude larger than the typical expected time constant for nonradiative trap-assisted recombination using the hole capture coefficient. The high hole mobility of Me-LPPP results in a large capture coefficient C_p of typically $\approx 1 \times 10^{-16}$ m^3 s^{-1}. Combined with a universal trap density of $\approx 5 \times 10^{23}$ m^{-3}, this would result in a relaxation time τ_r of only ≈30 ns. It should be noted that the use of a hole capture coefficient $C_p = (q/\varepsilon_0\varepsilon_r)\mu_p$ implicitly assumes that the slowest step in the trap-assisted recombination is the time that the hole needs to find the trapped electron. If, however, the recombination process itself is much slower than this time, this relation is not valid. In that case, it is also not possible to derive a trap concentration from the observed relaxation time. The observed relaxation time of 20 ms is therefore characteristic for a very slow trap-assisted recombination process. The fact that this observed relaxation time is in very good agreement with the life time reported for triplet emission in ladder-type polymers[32] is a further proof that the recombination observed at longer wavelength originates from trap-assisted triplet recombination.

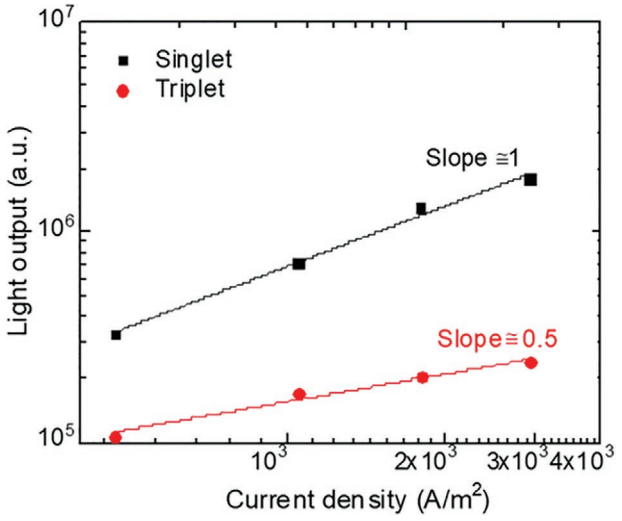

Figure 5. The light output of the singlet (2.4–2.8 eV) and triplet (1.8–2.2 eV) peaks as function of PLED current density.

2.4. Trap-Dilution

In PFO-based PLEDs, the singlet blue emission is often accompanied by a broad green emission band, originating from emissive ketone defects. The voltage dependence of the EL spectra demonstrated that the green emission has a trap-assisted origin.[10] A direct consequence of the trap-assisted nature of the green emission is that it is clearly visible in EL spectra, but far less pronounced in photoluminescence. It has recently

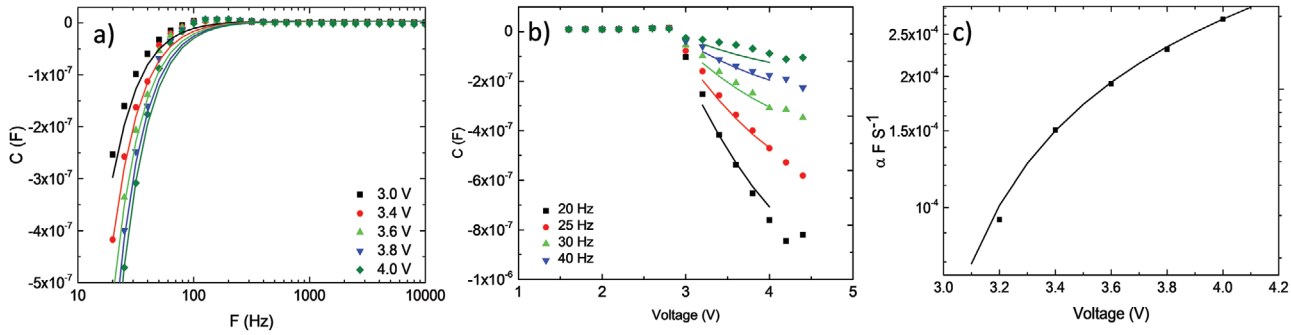

Figure 6. a) Differential capacitance C versus frequency at various bias voltages. The symbols represent the experimental data, while the solid lines are a fit to Equation (1) using $\tau_r = 20$ ms. b) C–V characteristics of a Me-LPPP PLED at different frequencies. c) $\alpha(V)$ values obtained from Equation (1) as a function of voltage.

been shown that trapping effects can be strongly suppressed by blending the semiconductor with a large band gap host.[24] In this initial study, polyvinylcarbazole (PVK) has been used as large band gap material. To demonstrate that the trap-dilution concept is fully independent of the semiconductive properties of PVK, PS also has been used as a large band gap host. It has been shown that trap-dilution also occurs when blending a semiconductor with the strongly insulating material PS, as long as intimate mixing of semiconductor and insulator is warranted.[33] Furthermore, trap dilution with PS nearly eliminates the contribution of emissive green trap-assisted recombination in the EL spectra of PFO.[10] As a final step, we therefore proceed with investigating the trap dilution effect using PS on the EL spectra of Me-LPPP-based PLEDs. **Figure 7** shows that upon increasing the PS content in the blend, a strong decline in the yellow-orange triplet emission occurs. For the Me-LPPP:PS blends with a 1:6 ratio, the EL spectrum is nearly equal to the PL spectrum of Me-LPPP in which the trap-assisted emission is absent. The suppression of the triplet emission as compared to the singlet emission by trap dilution is also consistent with the trap-assisted nature of the triplet emission in ME-LPPP. The fact that the triplet emission is trap-assisted also explains why in electroluminescence the triplet emission is far more pronounced as compared to photoluminescence and can even occur at room temperature.[10,16] As a result, trap dilution can be used to eliminate the negative effect of the triplet emission on the color purity of the EL spectra for blue Me-LPPP PLEDs.

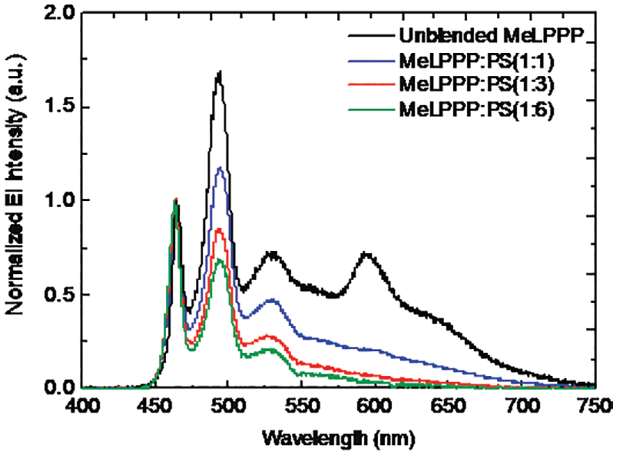

Figure 7. Electroluminescence spectra of PLEDs based on ≈120 nm active layers of unblended Me-LPPP and Me-LPPP:PS blends with various blend ratios. All spectra have been recorded at 8 V.

3. Conclusions

In conclusion, the hole transport in Me-LPPP is characterized by a trap-free space-charge limited current with a high mobility of 2×10^{-8} m² V^{-1} s^{-1} due to reduced energetic disorder. The electron transport is strongly trap-limited; additional traps are required on top of the universal trapping sites in order to explain the large difference between electron and hole currents. The EL spectrum shows next to the blue singlet peaks, additional features at longer wavelengths, including yellow-orange triplet emission. The triplet emission shows a weaker dependence on voltage as compared to the singlet emission and Me-LPPP PLEDs show a strongly pronounced negative capacitance governed by a long time constant of 20 ms. Both features indicate that the triplet emission is of trap-assisted nature, which is further confirmed by trap-dilution experiments.

4. Experimental Section

Materials: Me-LPPP was synthesized in a sequence of Suzuki-type polycondensation and subsequent post-polymerization cyclization according to literature ($\bar{M}_w$ = 51 kDa, PDI = 1.96).[12] As large band gap material for trap dilution, PS was used. The PS (atactic, $\bar{M}_w$ = 1.1 kDa, PDI = 1.15) was synthesized via anionic polymerization of styrene. Me-LPPP:PS blend solutions were prepared by dissolving the polymers in chloroform using weight ratios of 1:0, 1:1, 1:3, and 1:6. Films of the unblended conducting polymer and its blend with PS were applied using standard spin-coating methods.

Device Fabrication: The electron current through the polymer was measured on electron-only devices having a glass/Al (30 nm)/polymer/Ba (5 nm)/Al (100 nm) architecture. Here, Ba with a work function of 2.7 eV provides an ohmic contact for electron injection, since it aligns with the LUMO of Me-LPPP located at 2.7 eV below vacuum. For hole-only devices, the device structure glass/ITO/poly(3,4-ethylenedioxythiophene):poly(styrene sulfonic acid) (PEDOT:PSS) (Heraeus Clevios 4083)/polymer/MoO3 (10 nm)/Al (100 nm) was used. Here, an ohmic contact for hole injection was formed on Me-LPPP (HOMO level of 5.3 below vacuum)[34] by MoO3 that exhibited a work function of 6.9 eV. After deposition, the PEDOT:PSS was annealed at 140 °C. Subsequently, the

Me LPPP solution was deposited by spin coating. Finally, for PLEDs, the current was measured using the device structure glass/ITO/PEDOT:PSS/polymer/Ba/Al. The top contacts for hole-only devices MoO_3 (10 nm)/Al (100 nm) and for PLEDs Ba (5 nm)/Al (100 nm) were thermally evaporated.

Measurements: After device preparation, steady-state current–voltage measurements were performed in inert (N_2) atmosphere using a Keithley 2400 source meter. Light output was recorded with a calibrated Si photodiode, and electroluminescence spectra were recorded with a USB4000 UV–Vis–ES Ocean Optic spectrometer. Photoluminescence spectra were recorded with a TIDAS Mono RS232 spectrometer. Impedance data were taken using an Agilent 4284a LCR meter, with the modulation frequency swept from 20 Hz to 8×10^5 Hz at various voltages.

Supporting Information

Supporting Information is available from the Wiley Online Library or from the author.

Conflict of Interest

The authors declare no conflict of interest.

Keywords

charge transport, conjugated polymers, light-emitting diodes

Received: January 21, 2020
Revised: February 26, 2020
Published online: March 19, 2020

[1] R. H. Friend, R. W. Gymer, A. B. Holmes, J. H. Burroughes, R. N. Marks, C. Taliani, D. D. C. Bradley, D. A. Dos Santos, J. L. Brédas, M. Lögdlund, W. R. Salaneck, *Nature* **1999**, *397*, 121.
[2] M. T. Bernius, M. Inbasekaran, J. O'Brien, W. Wu, *Adv. Mater.* **2000**, *12*, 1737.
[3] A. J. Heeger, *Solid State Commun.* **1998**, *107*, 673.
[4] A. Kraft, A. C. Grimsdale, A. B. Holmes, *Angew. Chem., Int. Ed.* **1998**, *37*, 402.
[5] X. Zhang, S. A. Jenekhe, *Macromolecules* **2000**, *33*, 2069.
[6] A. P. Kulkarni, S. A. Jenekhe, *Macromolecules* **2003**, *36*, 5285.
[7] D. Kim, H. Cho, C. Kim, *Prog. Polym. Sci.* **2000**, *25*, 1089.
[8] D. Abbaszadeh, P. W. M. Blom, *Adv. Electron. Mater.* **2016**, *2*, 1500406.
[9] E. Khodabakhshi, P. W. M. Blom, J. J. Michels, *Appl. Phys. Lett.* **2019**, *114*, 093301.
[10] E. Khodabakhshi, J. J. Michels, P. W. M. Blom, *AIP Adv.* **2017**, *7*, 075209.
[11] H. Bässler, *Phys. Status Solidi B* **1993**, *175*, 15.
[12] U. Scherf, K. Müllen, *Makromol. Chem., Rapid Commun.* **1991**, *12*, 489.
[13] U. Lemmer, S. Heun, R. Mahrt, U. Scherf, M. Hopmeier, U. Siegner, E. O. Göbel, K. Müllen, H. Bässler, *Chem. Phys. Lett.* **1995**, *240*, 373.
[14] D. Hertel, U. Scherf, H. Bässler, *Adv. Mater.* **1998**, *10*, 1119.
[15] Y. V. Romanovskii, A. Gerhard, B. Schweitzer, U. Scherf, R. Personov, H. Bässler, *Phys. Rev. Lett.* **2000**, *84*, 1027.
[16] J. M. Lupton, A. Pogantsch, T. Piok, E. J. W. List, S. Patil, U. Scherf, *Phys. Rev. Lett.* **2002**, *89*, 167401.
[17] L. Romaner, L. G. Heimel, H. Wiesenhofer, P. Scandiucci de Freitas, U. Scherf, J.-L. Brédas, E. Zojer, E. J. W. List, *Chem. Mater.* **2004**, *16*, 4667.
[18] L. Liu, S. Qiu, B. Wang, W. Zhang, P. Lu, Z. Xie, M. Hanif, Y. Ma, J. Shen, *J. Phys. Chem. B* **2005**, *109*, 23366.
[19] B. Kobin, F. Bianchi, S. Halm, J. Leistner, S. Blumstengel, F. Henneberger, S. Hecht, *Adv. Funct. Mater.* **2014**, *24*, 7717.
[20] H. T. Nicolai, M. Kuik, G. A. H. Wetzelaer, B. De Boer, C. Campbell, C. Risko, J.-L. Brédas, P. W. M. Blom, *Nat. Mater.* **2012**, *11*, 882.
[21] W. F. Pasveer, J. Cottaar, C. Tanase, R. Coehoorn, P. A. Bobbert, P. W. M. Blom, D. M. De Leeuw, M. A. J. Michels, *Phys. Rev. Lett.* **2005**, *94*, 206601.
[22] R. Coehoorn, W. F. Pasveer, P. A. Bobbert, M. A. J. Michels, *Phys. Rev. B* **2005**, *72*, 155206.
[23] P. W. M. Blom, M. J. M. De Jong, J. J. M. Vleggaar, *Appl. Phys. Lett.* **1996**, *68*, 3308.
[24] D. Abbaszadeh, A. Kunz, G. A. H. Wetzelaer, J. J. Michels, N. I. Crăciun, K. Koynov, I. Lieberwirth, P. W. M. Blom, *Nat. Mater.* **2016**, *15*, 628.
[25] E. W. Snedden, R. Thompson, S. Hintschich, A. P. Monkman, *Chem. Phys. Lett.* **2009**, *472*, 80.
[26] M. Wyman, *Ph.D. Thesis*, University of Rochester New York **2016**.
[27] J. Partee, E. L. Frankevich, B. Uhlhorn, J. Shinar, Y. Ding, T. J. Barton, *Phys. Rev. Lett.* **1999**, *82*, 3673.
[28] M. A. Baldo, D. F. O'Brien, Y. You, A. Shoustikov, S. Sibley, M. E. Thompson, S. R. Forrest, *Nature* **1998**, *395*, 151.
[29] G. A. H. Wetzelaer, M. Kuik, H. T. Nicolai, P. W. M. Blom, *Phys. Rev. B* **2011**, *83*, 165204.
[30] J. R. Macdonald, in *Impedance Spectroscopy*, Wiley, New York **1987**, p. 90.
[31] Q. Niu, N. I. Crăciun, G. A. H. Wetzelaer, P. W. M. Blom, *Phys. Rev. Lett.* **2018**, *120*, 116602.
[32] S. A. Bagnich, H. Bässler, D. Neher, *J. Chem. Phys.* **2004**, *121*, 9178.
[33] A. Kunz, P. W. M. Blom, J. J. Michels, *J. Mater. Chem. C* **2017**, *5*, 3042.
[34] C. Schwarz, S. Tscheuschner, J. Frisch, S. Winkler, N. Koch, H. Bässler, A. Köhler, *Phys. Rev. B* **2013**, *87*, 155205.